

# Self-organized criticality occurs in non-conservative neuronal networks during 'up' states

Daniel Millman<sup>1</sup>, Stefan Mihalas<sup>1</sup>, Alfredo Kirkwood<sup>1,2</sup> and Ernst Niebur<sup>1,2</sup>★

**During sleep, under anaesthesia and *in vitro*, cortical neurons in sensory, motor, association and executive areas fluctuate between so-called up and down states, which are characterized by distinct membrane potentials and spike rates<sup>1–5</sup>. Another phenomenon observed in preparations similar to those that exhibit up and down states—such as anaesthetized rats<sup>6</sup>, brain slices and cultures devoid of sensory input<sup>7</sup>, as well as awake monkey cortex<sup>8</sup>—is self-organized criticality (SOC). SOC is characterized by activity 'avalanches' with a branching parameter near unity and size distribution that obeys a power law with a critical exponent of about  $-3/2$ . Recent work has demonstrated SOC in conservative neuronal network models<sup>9,10</sup>, but critical behaviour breaks down when biologically realistic 'leaky' neurons are introduced<sup>9</sup>. Here, we report robust SOC behaviour in networks of non-conservative leaky integrate-and-fire neurons with short-term synaptic depression. We show analytically and numerically that these networks typically have two stable activity levels, corresponding to up and down states, that the networks switch spontaneously between these states and that up states are critical and down states are subcritical.**

Self-organized criticality (SOC) characterizes the spread of forest fires<sup>11</sup>, earthquakes<sup>12</sup> and avalanches of idealized grains toppling down sandpiles<sup>13</sup>. Analogously, neuronal activity propagates in 'neuronal avalanches'<sup>14</sup>. Up- and down-state behaviour is also a network-level phenomenon: a high proportion of the neurons in large cortical areas alternate between states at the same time<sup>2,15–18</sup>. Whereas down states are quiescent<sup>19</sup>, up states have high synaptic and spiking activity<sup>5</sup>, resembling that of rapid eye movement sleep and wakefulness<sup>20</sup>. Differences in synaptic activity and neuronal responsiveness between up and down states suggest that avalanche behaviour differs as well.

A recent modelling study<sup>9</sup> demonstrated criticality in a conservative network of non-leaky integrate-and-fire neurons with short-term synaptic depression (STSD). On addition of voltage leak, however, networks required a compensatory current to remain critical. In a similar conservative network with depression and facilitation, the same group found two stable states, one critical and one subcritical<sup>10</sup>. Non-conservative networks of leaky integrate-and-fire (LIF) neurons also exhibit stable up and down states<sup>21</sup>, which can be obtained with STSD alone<sup>22</sup>. We therefore investigate whether critical behaviour occurs in either the up or down state in these non-conservative LIF/STSD systems.

Solving the Fokker–Planck equation for the probability density of the membrane potential in a mean-field approximation, we obtain an analytical solution for the branching parameter

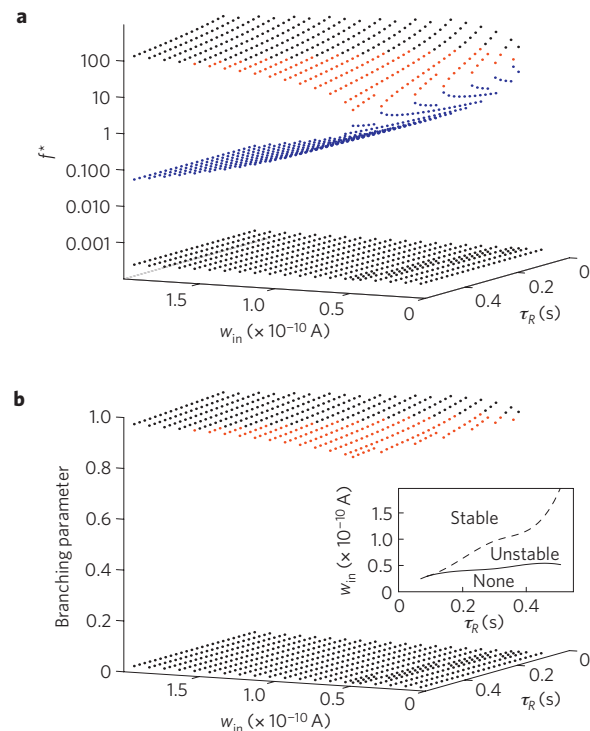


**Figure 1 | Bifurcations of mean-field approximation predict critical up states and subcritical down states.** **a**, Stable fixed points are shown in black, unstable fixed points in red and saddle nodes in blue. Quiescent stable down states are ubiquitous in the parameter region shown. When synapses are sufficiently strong and vesicle recovery is sufficiently fast, a stable or unstable high-activity up-state attractor emerges, as well as a saddle node at an intermediate firing rate. **b**, Analytical solution for the branching parameter of up and down states. Down states are subcritical with a branching parameter near zero, and the up states are critical with a branching parameter near unity. Inset: Two-dimensional view of different regions of up-state stability. Parameters:  $R = (2/3) \times 10^9 \Omega$ ,  $C = 3 \times 10^{-11} \text{ F}$ ,  $V_r = -70 \text{ mV}$ ,  $\theta = -50 \text{ mV}$ ,  $w_e = 95 \text{ pA}$ ,  $f_e = 5 \text{ Hz}$ ,  $\tau_s = 5 \text{ ms}$ ,  $\tau_p = 1 \text{ ms}$ ,  $n_r = 6$ ,  $n_s = 7.5$ ,  $p_r = 0.25$ .

during up and down states. The branching parameter is close to unity in the up state, indicating critical behaviour, and close to zero (subcritical) in the down state. Simulated networks of LIF neurons, just as biological neural systems, also have these properties. This behaviour is observed even as

<sup>1</sup>Zanvyl Krieger Mind/Brain Institute, Johns Hopkins University, Baltimore, Maryland 21218, USA, <sup>2</sup>Department of Neuroscience, Johns Hopkins University, Baltimore, Maryland 21218, USA. ★e-mail: niebur@jhu.edu.

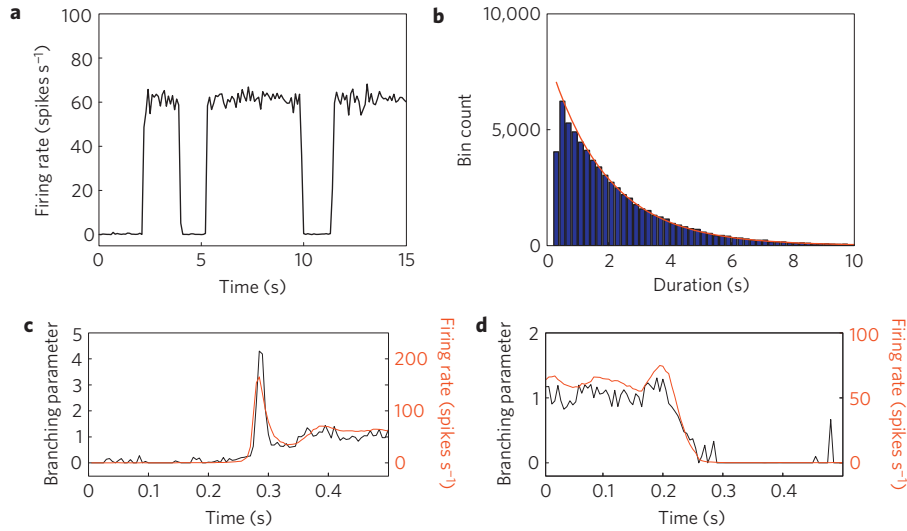


**Figure 2 | Simulated networks exhibit up- and down-state behaviour.** **a**, Networks spontaneously alternate between quiescent spiking (down state) and  $\sim 65 \text{ spikes s}^{-1}$  (up state). **b**, The up-state duration distribution is fitted well by an exponential (red line,  $\tau = 1.9 \text{ s}$ ). **c**, At down-to-up transitions, the branching parameter increases from zero and overshoots unity before settling near unity; the firing rate likewise overshoots. **d**, The branching parameter and firing rate decay towards zero at up-to-down transitions. The same parameters as Fig. 1,  $\tau_R = 100 \text{ ms}$ ,  $w_{in} = 50 \text{ pA}$ ; networks of 300 neurons.

additional biologically realistic features, including small-world connectivity, NMDA (N-methyl-D-aspartate) receptor currents and inhibition, are introduced.

We model networks of LIF neurons with excitatory synapses and STSD. Each neuron forms synapses with on average  $n_s$  other neurons with uniform probability. Also, each neuron receives Poisson external input at rate  $f_e$ . Glutamatergic synaptic currents of the  $\alpha$ -amino-3-hydroxy-5-methyl-4-isoxazole propionic acid (AMPA) receptor type from other neurons,  $I_{in}^i(t)$ , and external inputs,  $I_e^i(t)$ , are modelled as exponentials with amplitude  $w$  and integration time constant  $\tau_s$ ,

$$I_{in/e}^i(t) = w_{in/e} e^{-(t-t_s^i)/\tau_s} \quad (1)$$

In agreement with physiology, each synapse has multiple ( $n_r$ ) release sites. When a neuron fires spike  $i$  (at time  $t_s^i$ ), only some sites have a docked ‘usable’ vesicle. A usable site releases its vesicle with probability  $p_r$ , causing a postsynaptic current, equation (1). To model STSD,  $p_r$  is scaled by a factor,  $U_j(t)$ , that is zero immediately after a release at site  $j$ , at time  $t_r^j$ , and recovers exponentially with time constant  $\tau_R$ . Neuronal membranes have potential  $V$ , resting potential  $V_r$ , resistance  $R$  and capacitance  $C$ . On reaching threshold ( $\theta$ ), the potential resets to  $V_r$  after refractory period  $\tau_{rp}$ . The network dynamics are:

$$\dot{V} = -\frac{V - V_r}{RC} + \frac{1}{C} \left( \sum_i I_e^i(t) + \sum_i \sum_j H(p_r U_j(t_s^i) - \zeta) I_{in}^i(t) \right) \quad (2)$$

$$U_j(t) = 1 - e^{-\frac{(t-t_r^j)}{\tau_R}} \quad (3)$$

$$\text{if } V > \theta, \text{ then } V \rightarrow V_r \text{ after } \tau_{rp} \quad (4)$$

where  $\zeta$  is a random variable uniformly distributed on  $[0, 1]$ , and  $H(x)$  is the Heaviside step function.

The time derivative of mean synaptic utility,  $u(t) = \langle U_j(t) \rangle_j$ , can be expressed analytically (see the Methods section):

$$\dot{u} = \frac{1-u}{\tau_R} - up_r f \quad (5)$$

Furthermore, the probability distribution of subthreshold membrane potentials,  $P(V, t)$ , can be modelled as a diffusion–drift

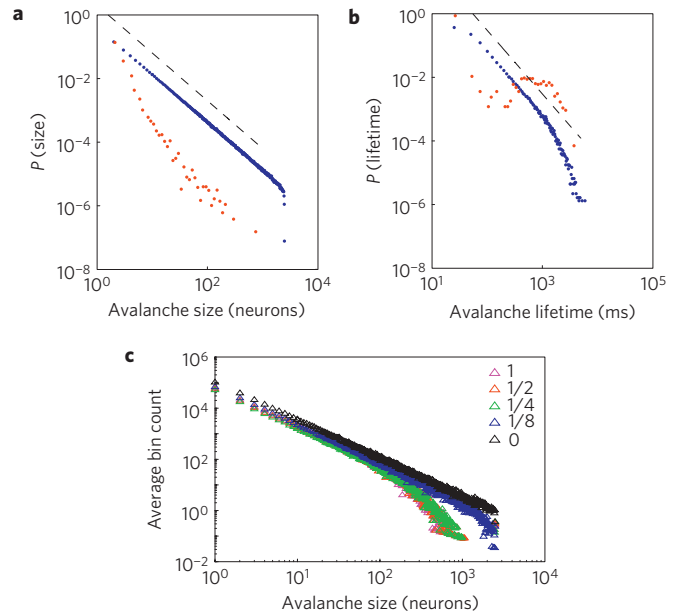


**Figure 3 | Up states are critical, down states are subcritical.** **a**, The frequency distribution of avalanche size (number of neurons) in the up state (blue) follows a power law with slope  $-1.5$  (dashed line), indicative of critical networks. In the down state (red), the distribution is not linear and few avalanches of size greater than 10 occur, indicative of subcritical networks. **b**, Similarly, the distribution of avalanche lifetimes follows a power law with slope  $-2.0$  (dashed line) in the up state (blue) but not the down state (red). The same model parameters as Fig. 2; networks of 2,500 neurons. **c**, Avalanche size distributions for networks with AMPA and NMDA excitatory currents and different amplitudes of inhibitory currents. The amplitude of inhibitory to excitatory synapses ( $w_{ltoE}$ ) is given in the legend as a fraction of the excitatory current amplitude. At the highest levels of inhibition, power laws begin to break down near system size. See Supplementary Data S2.5 for model details.

equation<sup>23</sup>. The drift, with velocity  $v_d(u, f, V)$ , results from the net change in potential owing to synaptic inputs minus the leak. Diffusion,  $D(u, f)$ , arises because synaptic inputs occur with

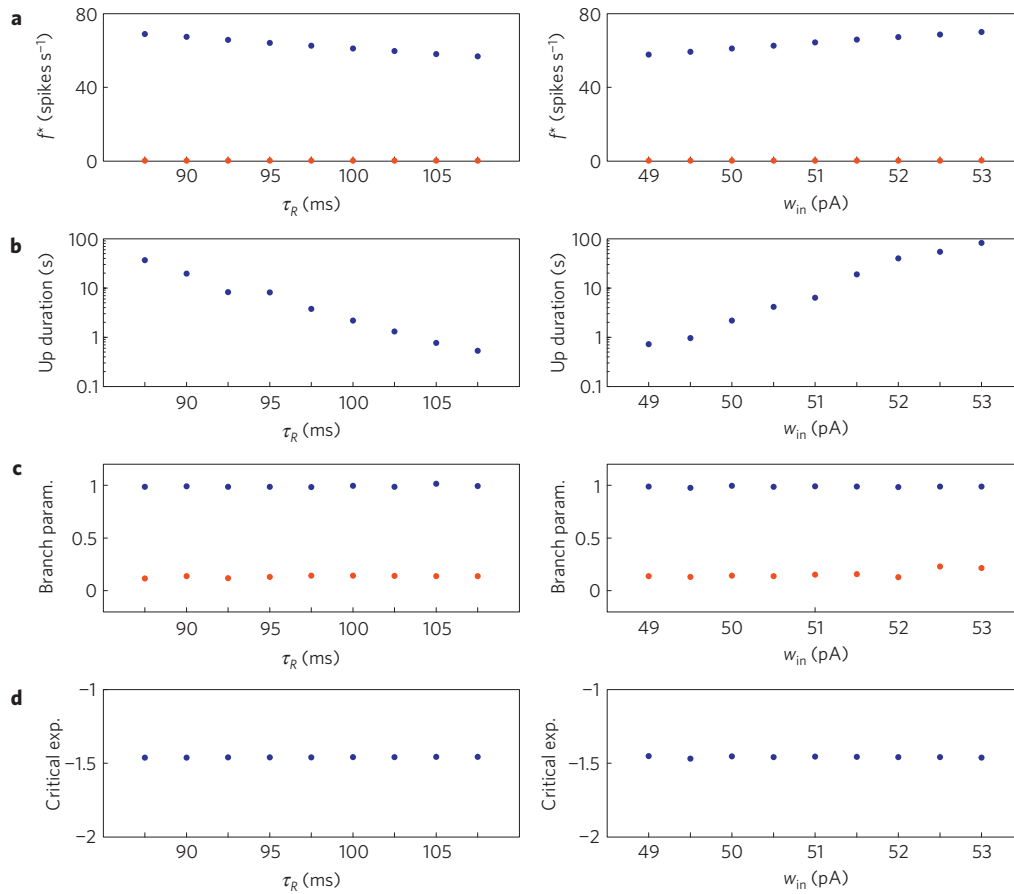


**Figure 4 | Criticality of up states and subcriticality of down states are robust to variations of crucial model parameters.** **a**, Up-state (blue) firing rates change slightly as  $\tau_R$  and  $w_{in}$  are changed; down states (red) remain quiescent. **b**, Up-state durations vary widely with changes in these parameters. **c**, Up- and down-state branching parameters remain near unity and zero, respectively, over these parameter regions. **d**, The up-state avalanche-size critical exponent remains near  $-1.5$ .

Poisson-like, rather than uniform, timing. The Fokker–Planck equation for the probability density of  $V$  is,

$$\frac{\partial P(V, t)}{\partial t} = D(u, f) \frac{\partial^2 P(V, t)}{\partial V^2} - \frac{\partial [v_d(u, f, V)P(V, t)]}{\partial V} \quad (6)$$

$$D(u, f) = \frac{1}{2} (V_e^2 f_e + n_s u^2 V_{in}^2 f) \quad (7)$$

$$v_d(u, f, V) = V_e f_e + n_s u V_{in} f - \frac{V - V_r}{RC} \quad (8)$$

where  $V_e = w_e \tau_s / C$  and  $V_{in} = p_r n_r w_{in} \tau_s / C$ , respectively, the mean instantaneous changes in membrane potential resulting from a single external and internal input event.

The firing rate is the probability current that passes through threshold:

$$f(t) = -D(u, f) \frac{\partial P(\theta, t)}{\partial V} \quad (9)$$

We calculate the time derivative of  $u$  analytically and of  $f$  numerically (Supplementary Methods S1.1) to analyse fixed points of the dynamical system. For typical parameter values for cortical neurons<sup>24,25</sup>, the system contains two stable fixed points, a quiescent down state with maximal synaptic utility and an up state with depressed synaptic utility, separated by a saddle node that sends trajectories to either stable state along the unstable manifold (Fig. 1a).

Networks with weak synapses (small  $w_{in}$ ) exhibit only a quiescent down state ( $f \approx 0$  spikes  $s^{-1}$ ). An unstable up state and a saddle node emerge with slightly stronger synapses, and with strong synapses the up state becomes stable. Increasing  $w_{in}$  further decreases the firing rate of the saddle node, thereby constricting the basin of attraction for the down state and making the up state the dominant feature. When vesicle replenishment is fast (short  $\tau_R$ ), the up-state firing rate is high. As replenishment becomes slower, the up-state firing rate decreases, then the up state becomes unstable and ultimately collides with the saddle node at a saddle-node bifurcation. Beyond the bifurcation, networks do not recover from STSD rapidly enough to sustain up states.

The branching parameter, the average number of neurons that one neuron is able to activate during an avalanche, is equal to the probability that the membrane potential of a postsynaptic neuron will cross threshold as a result of one input, times the number of postsynaptic neurons to which a neuron connects. As the influence of any given synapse on a cortical neuron is small, the integral can be approximated by the slope near threshold.

$$\sigma = n_s \int_{\theta - \epsilon}^{\theta} P(V, \infty) dV \approx -\frac{n_s \epsilon^2}{2} \frac{\partial P(\theta, \infty)}{\partial V} \quad (10)$$

where  $\epsilon := u V_{in} \ll (\theta - V_r)$  is the strength of a synapse. This can be expressed in terms of the firing rate at stable states (see the Methods section),  $f^*$ :

$$\sigma = \frac{n_s V_{in}^2 f^*}{V_e^2 f_e (1 + p_r \tau_R f^*)^2 + n_s V_{in}^2 f^*} \quad (11)$$

The analytical solution shows that (quiescent) down states are subcritical, and (active) up states are critical (Fig. 1b). In down states, external input dominates total synaptic input and the branching parameter approaches zero, indicative of subcritical networks. In up states, input from other neurons within the network dominates synaptic input, the branching parameter approaches unity and the network is critical.

We simulated networks of neurons described in Equations (2)–(4), using a generalized linear LIF model<sup>26</sup>. The networks spontaneously alternate between two distinct levels of firing corresponding to up and down states (Fig. 2a). Our analytical solution for the branching parameter is in close agreement with simulations for instantaneous synaptic voltage steps assumed in ref. 23 (Supplementary Data S2.1). To increase biological realism, we also modelled exponential synaptic currents and we obtained up and down states that persist for simulated seconds, which is consistent with findings in cortex<sup>27</sup>. In agreement with previous findings<sup>2,21</sup>, up-state durations are exponentially distributed (Fig. 2b; see Supplementary Data S2.2 for up-state interspike interval distribution).

The branching parameter follows the firing rate at state transitions. At down-to-up transitions, the branching parameter increases from zero and overshoots unity as activity spreads before finally settling near unity (Fig. 2c). At up-to-down transitions, the branching parameter decays with the firing rate towards zero (Fig. 2d). See Supplementary Data S2.3 for further discussion of state transitions.

Each up or down state was composed of hundreds or thousands of avalanches. Avalanche size and lifetime distributions in the up state follow power laws with critical exponents near  $-1.5$  and  $-2.0$  (Fig. 3a,b; maximum likelihood estimators:  $-1.50$  and  $-2.03$ ; verified by Kolmogorov–Smirnov tests with the method described in ref. 28), respectively. Avalanche distributions in the down state drop off rapidly such that few avalanches of size greater than 10 occur. We then increased the biological realism of our networks by introducing small-world connectivity (Supplementary Data S2.4), glutamatergic synapses of the NMDA type and inhibitory currents (Fig. 3c; Supplementary Data S2.5). Although NMDA receptor alone failed to reduce up-state firing rates to biological values, adding inhibition reduced the rates markedly (purely excitatory:  $64.0$  spikes  $s^{-1}$ ; 1I:8E:  $35.6$  spikes  $s^{-1}$ ; 1I:4E:  $8.7$  spikes  $s^{-1}$ ; 1I:2E:  $8.7$  spikes  $s^{-1}$ ; 1I:1E:  $8.4$  spikes  $s^{-1}$ ). In all of these conditions up states are critical and down states are subcritical, except for the highest levels of inhibition in which the power law in avalanche size distribution begins to break down near system size.

Finally, we inspect the robustness of these results by varying crucial model parameters. Whereas up-state firing rates change only slightly with changes in  $w_{in}$  and  $\tau_R$  (Fig. 4a), up-state durations vary widely (Fig. 4b). In all cases, the branching parameter remains near unity in the up state and near zero in the down state (Fig. 4c) and the up-state critical exponent near  $-1.5$  (Fig. 4d). See Supplementary Data S2.6 and S2.7 for further parameters.

In this contribution, we bring together two phenomena of complex networks that have been observed experimentally in neural systems: self-organized criticality and up- and down-state behaviour. We predict that biological up and down states are fundamentally different from a dynamical systems perspective: up states are critical and down states are subcritical. Up states achieve criticality because (1) a high firing rate ensures that avalanches propagate through the system faster than new avalanches are initiated ( $f_e \ll f^*$ ), and (2) activity is maintained at a constant level by compensating for leaks with an equivalent amount of synaptic input, arising primarily from recurrent activation, which makes the system temporarily quasi-conservative on average.

Memory consolidation is hypothesized to take place during sleep<sup>29</sup>, in which hippocampal and neocortical up and down states

are phase-locked<sup>18</sup>. This process may be enhanced during critical up states, when information transmission<sup>7</sup> and storage<sup>30</sup> approach their theoretical maxima.

## Methods

**Analytical solution for synaptic utility  $\hat{u}$ .** The time derivative of the mean synaptic utility is the sum of the rate of recovery and the rate of depression,  $\dot{u} = k_R + k_D$ . Recovery happens between releases and the average rate can be obtained from the time derivative of equation (3),

$$\frac{dU_j(t)}{dt} = \frac{\exp(-\frac{t-t_j}{\tau_R})}{\tau_R} = \frac{1-U_j(t)}{\tau_R} \quad (12)$$

$$k_R = \frac{d\langle U_j(t) \rangle}{dt} = \frac{1-\langle U_j(t) \rangle}{\tau_R} = \frac{1-u}{\tau_R} \quad (13)$$

to yield the first term on the right-hand side of equation (5).

A release site fully depletes following a vesicle release, which happens with probability  $p_r$  for each spike (which occur at rate  $f$ ). Thus, the average rate of depletion is,

$$k_D = -up_r f \quad (14)$$

yielding the second term on the right-hand side of equation (5).

**Analytical solution for the branching parameter  $\sigma$ .** We approximate the branching parameter at fixed points ( $u^*, f^*$ ) using the slope near threshold from equation (10)

$$\sigma = -\frac{n_s \epsilon^2}{2} \frac{\partial P(\theta, \infty)}{\partial V} \quad (15)$$

where  $\epsilon = uV_{in} \ll (\theta - V_r)$  was defined after equation (10), and we know the stationary firing rate from equations (8) and (9)

$$f_{stat} = -D(u^*, f^*) \frac{\partial P(\theta, \infty)}{\partial V} = -\frac{1}{2} (V_e^2 f_e + n_s u^{*2} V_{in}^2 f^*) \frac{\partial P(\theta, \infty)}{\partial V} \quad (16)$$

Solving for  $\partial P(\theta, \infty)/\partial V$  in equation (16) and inserting it into equation (15) yields

$$\sigma = \frac{n_s u^{*2} V_{in}^2 f_{stat}}{V_e^2 f_e + n_s u^{*2} V_{in}^2 f^*} \quad (17)$$

In addition, the  $u$ -nullcline can be calculated analytically from equation (5) to yield  $u^*$  in terms of  $f^*$ :

$$u^* = \frac{1}{1 + p_r \tau_R f^*} \quad (18)$$

Combining equations (17) and (18), and noting that  $f_{stat} = f^*$  at fixed points, we obtain equation (11), the analytical solution for the branching parameter at fixed points.

**Two distinct stable states.** Up and down states were established along two criteria of the firing rate: bimodality and contiguity. Hartigan's dip test was carried out on the firing-rate histograms to test for bimodality; the firing-rate histogram is bimodal ( $p$ -value = 0.015). Thus, we refer to time bins with a mean firing rate  $< 5$  spikes  $s^{-1}$  as being in the down state and those with rates greater than 5 spikes  $s^{-1}$  as being in the up state. To establish that 'states' are contiguous in time, which we consider the equivalent of stability from the mean-field approximation, we calculated whether firing rates remained at distinct levels for more consecutive time bins than expected by chance. Take the proportion of time bins in the up state to be  $p$  and in the down state to be  $1-p$ . Therefore, the binomial probability that consecutive time bins are in the same state is  $p^2 + (1-p)^2$  and the probability that they differ is  $2p(1-p)$ . The probability of  $N$  total time bins having  $X_0$  or more consecutive pairs in the same state is,

$$P(X > X_0) = \sum_{i=X_0}^{N-1} \binom{N-1}{i} (p^2 + (1-p)^2)^i (2p(1-p))^{N-1-i} \quad (19)$$

We find that the probability of obtaining the observed number of consecutive time bins in the same state is significantly smaller than expected if bins were independent, with significance  $P < 10^{-308}$  (the smallest possible number in the double-precision floating representation we use). For the up-state duration histogram, we plot only states that are maintained for more than 200 ms. Thus, networks remain in one state for more consecutive time bins than expected by chance before spontaneously switching to the other state.

**Avalanches.** Spatiotemporal activity is characterized in terms of neuronal avalanches. By definition a new avalanche is initiated when a background (external)

input is the first input to drive the membrane potential of a neuron above threshold. If, however, the membrane potential of a neuron first surpasses threshold as a result of a synaptic input from an existing avalanche member, then that neuron is considered a member of the same avalanche.

The branching parameter is defined as the average number of neurons activated directly by the initiating avalanche member (that is, second generation of the avalanche). This measure is consistent with that used in other studies<sup>7</sup> and maintains a common metric for both large and small avalanches.

We follow the method presented in ref. 28 to statistically validate criticality. Briefly, we find the maximum likelihood estimators under the assumption that avalanche distributions follow either a power law or an exponential. We then generate random power-law and exponential distributions given the calculated maximum likelihood estimators to determine by bootstrap the probability of obtaining a Kolmogorov–Smirnov distance at least as great as the sample. In all cases, we fail to reject the null hypothesis that avalanche distributions are power-law-distributed (Kolmogorov–Smirnov test  $p$  values: 0.46 and 0.29 for avalanche size and lifetime, respectively), but we do reject the null hypothesis that the distributions are exponentially distributed ( $p$ -values  $< 0.01$  for avalanche size and lifetime).

Received 8 February 2010; accepted 21 July 2010; published online 5 September 2010

## References

- Stern, E. A., Kincaid, A. E. & Wilson, C. J. Spontaneous subthreshold membrane potential fluctuations and action potential variability of rat corticostriatal and striatal neurons *in vivo*. *J. Neurophysiol.* **77**, 1697–1715 (1997).
- Cossart, R., Aronov, D. & Yuste, R. Attractor dynamics of network UP states in the neocortex. *Nature* **423**, 283–288 (2003).
- Plenz, D. & Kitai, S. T. Up and down states in striatal medium spiny neurons simultaneously recorded with spontaneous activity in fast-spiking interneurons studied in cortex-striatum-substantia nigra organotypic cultures. *J. Neurosci.* **18**, 266–283 (1998).
- Steriade, M., Nunez, A. & Amzica, F. A novel slow ( $< 1$  Hz) oscillation of neocortical neurons *in vivo*: Depolarizing and hyperpolarizing components. *J. Neurosci.* **13**, 3252–3265 (1993).
- Shu, Y., Hasenstaub, A., Badoual, M., Bal, T. & McCormick, D. A. Barrages of synaptic activity control the gain and sensitivity of cortical neurons. *J. Neurosci.* **23**, 10388–10401 (2003).
- Gireesh, E. D. & Plenz, D. Neuronal avalanches organize as nested theta- and beta/gamma-oscillations during development of cortical layer 2/3. *Proc. Natl Acad. Sci. USA* **105**, 7576–7581 (2008).
- Beggs, J. M. & Plenz, D. Neuronal avalanches in neocortical circuits. *J. Neurosci.* **23**, 11167–11177 (2003).
- Petermann, T. *et al.* Spontaneous cortical activity in awake monkeys composed of neuronal avalanches. *Proc. Natl Acad. Sci. USA* **106**, 15921–15926 (2009).
- Levina, A., Herrmann, J. M. & Geisel, T. Dynamical synapses causing self-organized criticality in neural networks. *Nature Phys.* **3**, 857–860 (2007).
- Levina, A., Herrmann, J. M. & Geisel, T. Phase transitions towards criticality in a neural system with adaptive interactions. *Phys. Rev. Lett.* **102**, 118110 (2009).
- Malamud, B. D., Morein, G. & Turcotte, D. L. Forest fires: An example of self-organized critical behaviour. *Science* **281**, 1840–1842 (1998).
- Gutenberg, B. & Richter, C. F. *Seismicity of the Earth* (Princeton Univ. Press, 1956).
- Bak, P., Tang, C. & Wiesenfeld, K. Self-organized criticality: An explanation of  $1/f$  noise. *Phys. Rev. Lett.* **59**, 381–384 (1987).
- Plenz, D. & Thiagarajan, T. C. The organizing principles of neuronal avalanches: Cell assemblies in the cortex? *Trends Neurosci.* **30**, 101–110 (2007).
- Lampl, I., Reichova, I. & Ferster, D. Synchronous membrane potential fluctuations in neurons of the cat visual cortex. *Neuron* **22**, 361–374 (1999).
- Watson, B. O., MacLean, J. N. & Yuste, R. UP states protect ongoing cortical activity from thalamic inputs. *PLoS One* **3**, e3971 (2008).
- MacLean, J. N., Watson, B. O., Aaron, G. B. & Yuste, R. Internal dynamics determine the cortical response to thalamic stimulation. *Neuron* **48**, 811–823 (2005).
- Hahn, T. T. G., Sakmann, B. & Mehta, M. R. Phase-locking of hippocampal interneurons' membrane potential to neocortical up–down states. *Nature Neurosci.* **9**, 1359–1361 (2006).
- Cowan, R. L. & Wilson, C. J. Spontaneous firing patterns and axonal projections of single corticostriatal neurons in the rat medial agranular cortex. *J. Neurophysiol.* **71**, 17–32 (1994).
- Destexhe, A., Hughes, S. W., Rudolph, M. & Crunelli, V. Are corticothalamic UP states fragments of wakefulness? *Trends Neurosci.* **30**, 334–342 (2007).
- Parga, N. & Abbott, L. F. Network model of spontaneous activity exhibiting synchronous transitions between up and down states. *Front. Neurosci.* **1**, 57–66 (2007).
- Holcman, D. & Tsodyks, M. The emergence of up and down states in cortical networks. *PLoS Comput. Biol.* **2**, e23 (2006).
- Brunel, N. Dynamics of sparsely connected networks of excitatory and inhibitory spiking neurons. *J. Comput. Neurosci.* **8**, 183–208 (2000).
- Südhof, T. C. The synaptic vesicle cycle. *Annu. Rev. Neurosci.* **27**, 509–547 (2004).
- Dobrunz, L. E. & Stevens, C. F. Heterogeneity of release probability, facilitation, and depletion at central synapses. *Neuron* **18**, 995–1008 (1997).
- Mihalas, S. & Niebur, E. A generalized linear integrate-and-fire neural model produces diverse spiking behaviour. *Neural Comput.* **21**, 704–718 (2009).
- Amzica, F. & Steriade, M. Short- and long-range neuronal synchronization of the slow ( $< 1$  Hz) cortical oscillation. *J. Neurophysiol.* **73**, 20–38 (1995).
- Clauset, A., Shalizi, C. R. & Newman, M. E. J. Power-law distributions in empirical data. *SIAM Rev.* **51**, 661–703 (2009).
- Walker, M. P. & Stickgold, R. Sleep-dependent learning and memory consolidation. *Neuron* **44**, 121–133 (2004).
- Haldeman, C. & Beggs, J. M. Critical branching captures activity in living neural networks and maximizes the number of metastable states. *Phys. Rev. Lett.* **94**, 058101 (2005).

## Acknowledgements

The authors thank Y. Dong and V. M. K. Namboodiri for useful discussions, and Y. Dong for the use of a neuronal simulator package. Supported through NIH grants R01NS040596, R01EY016281 and 5R01EY012124 and ONR grant N000141010278.

## Author contributions

D.M., S.M., A.K. and E.N. planned the study. D.M. and S.M. carried out analytical work. D.M. carried out network simulations and analysis. D.M., S.M., A.K. and E.N. wrote the manuscript.

## Additional information

The authors declare no competing financial interests. Supplementary information accompanies this paper on [www.nature.com/naturephysics](http://www.nature.com/naturephysics). Reprints and permissions information is available online at <http://npg.nature.com/reprintsandpermissions>. Correspondence and requests for materials should be addressed to E.N.